J. Indones. Math. Soc.
Vol. 31, No. 01 (2025), pp. 1–12.

Simulation of Tsunami Waves Generated by Landslide Movements on a Flat Bottom

Rani Sulvianuri[1*], Glagah Eskacakra Setyowisnu[2], and Sri Redjeki Pudjaprasetya[3]

[1,2,3]Industrial and Financial Mathematics Research Group, Institut Teknologi Bandung, Indonesia

[1]ranisulvianuri@gmail.com, [2]setyowisnu99@gmail.com, [3]srpudjap@gmail.com

Abstract. Disasters like tsunamis are typically triggered by tectonic earthquakes, volcanic eruptions, or landslides. Tsunami waves can hit the coast with enormous energy, causing great damage. This study focuses on landslide-generated wave phenomena; the analytical formula of the linear dispersive model is adopted and used to simulate the development of free surface waves due to bottom landslides. Various types of landslide motion were simulated over a flat bottom depth and the resulting surface wave forms were examined and compared with the far-field leading wave type of solution. In addition, the effect of wave dispersion on the resulting wave pattern was investigated.

Key words and Phrases: Landslide tsunami, linear dispersive wave model, analytical solution.

1. INTRODUCTION

Tsunami is a natural disaster that can cause significant damage to coastal regions. They are most commonly triggered by tectonic earthquakes or volcanic eruptions, but can also be generated by landslides, as happened in Lituya Bay in 1964, Papua New Guinea in 1998, and Palu Bay in 2018. In recent years, there has been a growing interest in understanding the characteristics of tsunami waves generated by landslides, and the potential hazards they pose to coastal communities.

Several studies have been conducted related to landslide-generated tsunamis. One of the pioneering studies on this topic was carried out by Tinti et al. [1], which investigates the characteristics of surface waves caused by landslides moving

*Corresponding author

2020 Mathematics Subject Classification: 5Q35, 76B15.
Received: 06-01-2025, accepted: 23-02-2025.

along a flat bottom using a hydrostatic model. Furthermore, Whittaker et al. [2] examine in more detail the relationship between the speed of erosion and the amplitude of the resulting waves, as well as the behavior of the wave field. Studies related to numerical schemes of hydrostatic models to simulate the formation of waves generated by landslides can be found in Tjandra & Pudjaprasetya [3], see also Magdalena et al. [4]. A significant breakthrough was conducted by Lo & Liu in [5], who studied the analytical solutions of the fully dispersive model, as well as the weakly dispersive model, for landslides moving at constant speed at constant water depth. Furthermore, Jing et al. in [6] and [7] adopt fully and weakly dispersive models to examine waves resulting from landslides moving with constant acceleration. For studies of waves due to landslide over a sloping beach, readers are referred to [8] and [9].

In this paper, we present a study on the phenomenon of landslide-generated waves, with a focus on the development of free surface waves due to landslides over flat bottoms. The analytical formula of the linear dispersive model is considered and used to simulate the development of free surface elevation due to landslide. Simulations are conducted for various types of landslides. We also examine and investigate the effect of wave dispersion on the resulting surface wave forms. The discussion here is limited to the use of analytical solutions of the dispersive linear model, while for numerical modeling, the reader is referred to our other articles, for instance [10], and also [11]. For experimental studies, the reader is referred to [12], [13].

The paper is organized as follows. Section 2 discusses the governing equations in the form of a dispersive wave model, along with analytical solutions in terms of the inverse Fourier and Laplace transforms; with this analytical formulation, in Section 3, we discuss the steps used to simulate the development of free surface wave due to landslides. Section 4 presents the far-field leading wave solutions compared with free surface elevation produced by landslides of various shapes.

2. DISPERSIVE WAVE MODEL

In this section, we present a brief summary of the complete linear dispersive wave equations and outline the analytical solution that can be obtained through the use of Fourier and Laplace transforms as proposed by Jing, et al. [6].

Consider an ideal fluid layer bounded above by a free surface $\eta(x,t)$ and below by a bottom topography $z = B(x,t) - h_0$. Here, $B(x,t)$ represents the moving landslide on a constant water depth h_0. Let $\Phi(x,z,t)$ denote the velocity potential that satisfies the following governing equations consisting of the Laplace equation with three boundary conditions.

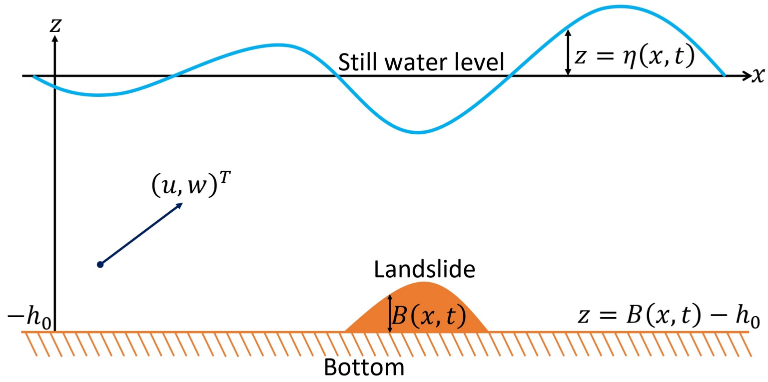

FIGURE 1. Sketch of fluid domain and notations

$$
\begin{aligned}
\Phi_{xx} + \Phi_{zz} &= 0, \qquad && x \in \mathbb{R},\ -h_0 < z < 0, && (1)\\
\eta_t &= \Phi_z, && z = 0, && (2)\\
\Phi_t + g\eta &= 0, && z = 0, && (3)\\
\Phi_z = B_t(x,t) &= F(x,t), && z = -h_0. && (4)
\end{aligned}
$$

In the description above, $B(x,t)$ represents the moving landslide that depends on time t, and in this study, we assume a solid landslide with constant speed.

The Fourier transform of a function $f(x)$ is indicated using a tilde as follows

$$\tilde{f}(k) = \int_{-\infty}^{\infty} f(x)e^{-ikx}dx,\ \ f(x) = \frac{1}{2\pi}\int_{-\infty}^{\infty} \tilde{f}(k)e^{ikx}dk,$$

whereas the Laplace transform of a function $g(t)$ is indicated using a bar

$$\bar{g}(s) = \int_{0}^{\infty} g(t)e^{-st}dt,\ \ g(t) = \frac{1}{2\pi i}\int_{\Gamma} \bar{g}(s)e^{st}ds.$$

By using the Fourier transform with respect to the spatial variable x and the Laplace transform with respect to the time variable t, Equation (1) is transformed into an ordinary differential equation that can be solved. Using three boundary conditions, the particular solution can then be determined as follows.

$$\bar{\tilde{\Phi}}(k,s) = \frac{\bar{\tilde{F}}(k,s)}{k}\frac{s^2\sinh(kz) - gk\cosh(kz)}{s^2\cosh(kh_0) + gk\sinh(kh_0)} \tag{5}$$

where $\bar{\tilde{F}}(k,s) = \int\limits_{-\infty}^{\infty} e^{-ikx} \left(\int\limits_{0}^{\infty} e^{-st} B_t(x,t)dt \right) dx$, see [6] for details. The transforming surface can be obtained from the dynamic boundary conditions

$$\bar{\tilde{\eta}}(k,s) = \frac{1}{\cosh{(kh_0)}} \frac{s\bar{\tilde{F}}(k,s)}{s^2+\omega^2}$$

where

$$\omega^2 = gk\tanh(kh_0) \tag{6}$$

is the dispersion relation. We obtain the following by taking the inverse of the Fourier and Laplace transforms.

$$\eta(x,t) = \frac{1}{2\pi} \int\limits_{-\infty}^{\infty} \frac{e^{ikx}}{\cosh kh_0} \int\limits_{0}^{t} \tilde{F}(k,\tau)\cos[\omega(t-\tau)]d\tau dk. \tag{7}$$

Restrict to a solid landslide $B(x,t) = B(x - x_0(t))$, with $x_0(t)$ as the center of the landslide. Then $\tilde{F}(k,\tau)$ becomes

$$\tilde{F}(k,t) = \int\limits_{-\infty}^{\infty} e^{-ikx} \frac{\partial B}{\partial t} dk = (-ik)\frac{dx_0}{dt}\tilde{B}(k)e^{-ikx_0}. \tag{8}$$

Due to landslide movement on the bottom, the initially still water level will deform, causing surface waves to develop. The linear dispersive model predicts the free surface dynamics according to (7). It is worth noting that if the function B representing the landslide form is known, then it suffices to compute the Fourier transform of said function, resulting in $\tilde{F}$. Utilizing $\tilde{F}$ allows for the calculation of the elevation of the free surface. In the next section, we will discuss the steps to simulate the dynamics of wave surfaces using Matlab.

3. LANDSLIDE GENERATED WAVES IN CONSTANT DEPTH

In this section, the analytical formula (7) is used to simulate the development of free surface waves due to landslide motion. Although the analytical formula is explicit, it consists of a double improper integral and a Fourier-transformed function. We employ a computer programming language (Matlab) to calculate them, since it is not trivial here we describe the steps.

(1) Set time $t = t_n$ at which the free surface will be plotted.
(2) Find the Fourier transform formula of the landslide $\tilde{B}_j(k)$ for the corresponding landslide B_j. The index 'j' indicates the type of landslide that will be used later on.
(3) For a landslide that moves with constant speed V, the position of the landslide center at any time is $x_0(t) = Vt$, and the Fourier transform $\tilde{F}_j(k,t)$ can be calculated using (8).

(4) The surface $\eta(x, t_n)$ is calculated using a double integral according to the formula (7), with the dispersion $\omega(k)$ follows from (6).

Several notes indicate that the formula obtained (7) has an integral form on an infinite number of wave numbers, k. However, when performing numerical integration with Matlab, we need to provide finite bounds for the integral. We have tried several intervals, that is $-20 < k < 20$, $-30 < k < 30$, $-40 < k < 40$, and $-100 < k < 100$ but we found that they give nearly the same results, therefore we use $-20 < k < 20$ for most calculations. Our software calculates the integral using the adaptive quadrature method, and an absolute error of $1e-5$. Furthermore, the integral with respect to k should avoid all singularities of the integration, in this singularity case of $\tilde{B}_j(k)$.

First, we simulate a landslide moving at a constant speed $V = 0.5$ m/sec on a flat bottom with depth $h_0 = 0.25$ m. For this simulation, we used a Gaussian landslide of amplitude A m.

$$B_1(x - Vt) = Ae^{-8(x-Vt)^2} \tag{9}$$

and the Fourier transform is

$$\tilde{B}_1 = A\frac{\sqrt{2\pi}}{4}e^{-(1/32)k^2}e^{-ikVt} \tag{10}$$

For this simulation, we normalized the wave celerity $\sqrt{gh_0}$ to one. Also, it should be noted that all parameters utilized in this simulation have been normalized. The numerical result is shown in Figure 2.

Due to landslide movement on the bottom, the initially zero surface is deformed, and the resulting free surface at several subsequent times $t = 0.5$ sec, $t = 1.0$ sec and $t = 2.0$ sec, are plotted in Figure 2. This simulation serves as a validation of the general solution (7). As can be seen in Figure 2 the surface plots show good agreement with analytical solutions of the same case as proposed by [5].

Following the theoretical prediction described in [5], the surface consists of three wave components: $\eta_+(x, t)$ with a positive phase moving to the right with velocity $\sqrt{gh_0}$, $\eta_-(x, t)$ with a negative phase moving to the left with velocity $-\sqrt{gh_0}$, and the third wave $\eta_V(x, t)$ with a negative phase moving to the right with the velocity of landslide V.

If $V < \sqrt{gh_0}$, after a sufficient amount of time the two waves moving to the right will be quite far apart. The leading wave, namely $\eta_+^*(x, t)$ is known as the far-field leading wave. A more detailed discussion regarding the far-field leading wave will be presented in the following section.

4. FAR-FIELD LEADING WAVE SOLUTION

Far-field leading wave is the behavior of the first wave crest in the region far from the wave source. The far-field leading wave is essential for understanding the

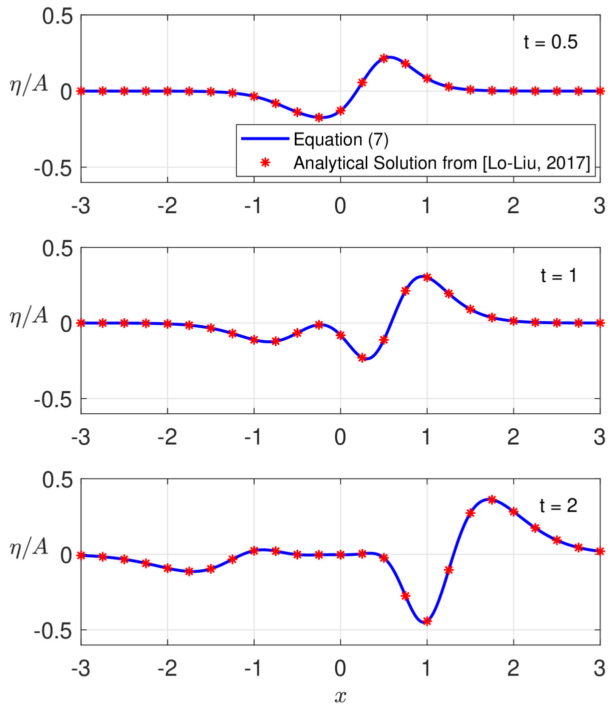

FIGURE 2. Surface elevation $\eta(x,t)/A$ at subsequent times $t = 0.5$ sec, $t = 1.0$ sec, and $t = 2.0$ sec, due to a Gaussian landslide at a flat depth $h_0 = 0.25$ m moving at speed $V = 0.5$ m/sec

behavior of water waves at long distances from their source, such as in the open ocean. In this section, we examine the phenomenon of this far-field leading wave in more detail. For solid landslides with amplitude A moving at a constant speed V will generate surface waves, and the solution for the far-field leading wave is provided in [14] as follows:

$$\eta_+^*(x,t) = \frac{AV}{2(\sqrt{gh_0}-V)}\left\{S\xi^{1/3}Ai\,(\sigma) - M_1\xi^{2/3}Ai'\,(\sigma) + \frac{M_2}{2}\xi Ai''\,(\sigma)\right\} + ... \quad (11)$$

$$\sigma = \xi^{1/3}\frac{x-\sqrt{gh_0}t}{L}, \quad \xi = \left(\frac{2L}{\mu^2\sqrt{gh_0}t}\right), \quad \mu = \frac{h_0}{L}. \quad (12)$$

The formula (11) is written in physical variables, with L represents the characteristic length of the landslide, and the non-dimensional parameter $\mu = h_0/L$ that represents the dispersion effect. Further observation of solution (11), the first, second, and third terms depend respectively on S the area enclosed by the landslide, M_1 the first moment, and M_2 the second moment. Moreover, for a positive landslide hump ($S > 0$), the first moment $M_1 = Sx_c$, with x_c center of mass of the landslide. Therefore, the first two terms of the far-field leading wave (11) depend on the area of the landslide. In the following, we will simulate several forms of landslides with the same enclosed area. We focus on three shapes: a Gaussian (9), a rectangular, and a triangular, with explicit formulas as follows.

$$B_2(x - Vt) = A\left(H\left(x - Vt + \frac{\sqrt{2\pi}}{8}\right) - H\left(x - Vt - \frac{\sqrt{2\pi}}{8}\right)\right), \tag{13}$$

$$\begin{aligned} B_3(x - Vt) = A&\left[1 + \frac{4}{\sqrt{2\pi}}(x - Vt)\right]\left[H\left(x - Vt + \frac{\sqrt{2\pi}}{4}\right) - H(x - Vt)\right] \\ &+ A\left[1 - \frac{4}{\sqrt{2\pi}}(x - Vt)\right]\left[H(x - Vt) - H\left(x - Vt - \frac{\sqrt{2\pi}}{4}\right)\right]. \end{aligned} \tag{14}$$

The following is the Fourier transformation of (13) and (14)

$$\tilde{B}_2 = i\frac{A}{k}(e^{-i(\sqrt{2\pi}/8)k} - e^{i(\sqrt{2\pi}/8)k})e^{-ikVt} \tag{15}$$

$$\tilde{B}_3 = A\frac{2\sqrt{2}}{\sqrt{\pi}k^2}(2 - e^{-i(\sqrt{2\pi}/4)k} - e^{i(\sqrt{2\pi}/4)k})e^{-ikVt} \tag{16}$$

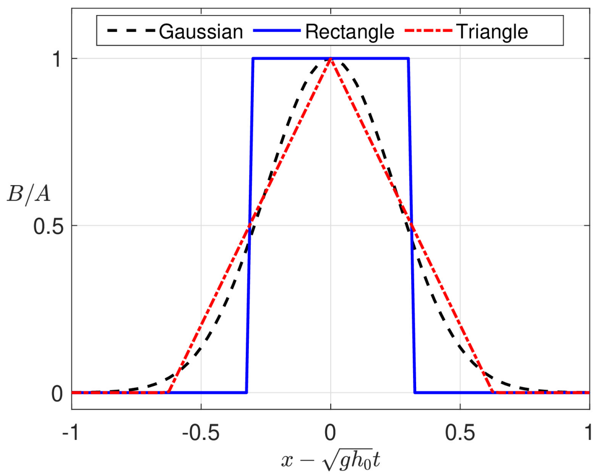

FIGURE 3. Three different landslide shapes, all of the same height and having the same enclosed area

These three forms of landslides will be simulated and compared with the far-field leading wave solution. As will be shown in the following sections, landslides of different shapes but have the same enclosed areas, i.e. B_1, B_2, B_3, will generate an identical leading surface wave; this phenomenon can be observed after a sufficiently long observation time. Thus, this is in accordance with far-field theory.

4.1. **Case $h_0 = 0.25$ m.**

We consider three forms of solid landslides (9), (13), and (14) that move with constant velocity V over a flat bottom h_0. This simulation uses parameters $V = 0.5$ m/sec, $g = 9.81$ m/sec^2, and $h_0 = 0.25$ m. Here we introduce the normalized time variable t^* as follows $t^* = t\sqrt{gh_0}/L$, with t the physical time variable. Together with the far-field leading wave solution, simulation results are plotted at subsequent (normalized) times t^*, see Figure 4. As shown in this figure, all three landslide-generated waves have similar profiles. For the surface plot at time $t^* = 10.0$ some deviation occurs, however, the leading wave still follows the far-field analytical solution.

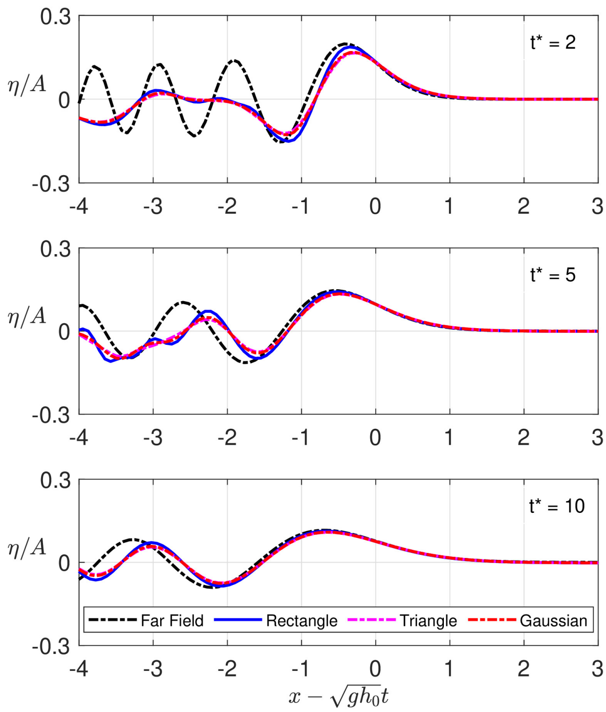

FIGURE 4. Surface elevation $\eta(x,t)/A$ generated by landslides at subsequent times $t^* = \{2.0, 5.0, 10.0\}$, due to Gaussian landslide B_1, rectangular landslide B_2, and triangular landslide B_3, and far-field solution (11) on a flat depth $h_0 = 0.25$ m

4.2. Case $h_0 = 0.4$ m.

Similar to the previous, here calculations were conducted using the same parameters, but using water depth $h_0 = 0.4$ m. Figure 5 shows the comparison of $\eta(x,t)/A$ solution (7) and far-field solution (11). We can see that the free surface responds differently due to the different landslide shapes; however, as time progresses, the leading waves converge. After a sufficiently long observation time, all three landslides produce the same leading wave as predicted by the far-field analytical solution and thus confirm the far-field theory.

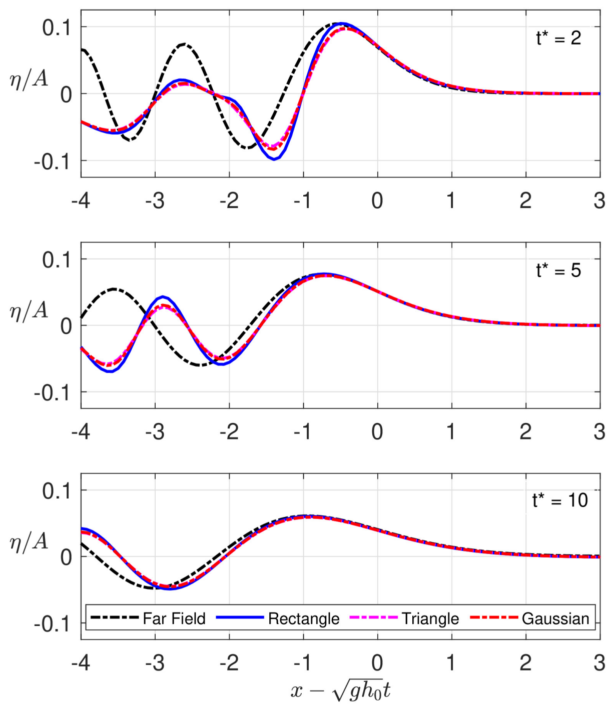

FIGURE 5. Surface elevation $\eta(x,t)/A$ generated by landslides at subsequent times $t^* = \{2.0, 5.0, 10.0\}$, due to Gaussian landslide B_1, rectangular landslide B_2, and triangular landslide B_3, and far-field solution (11) on a flat depth $h_0 = 0.4$ m

4.3. The effect of the dispersion parameter μ.

All landslides discussed here have a typical length $L = 1$ m, and hence the dispersion parameter depends solely on water depth h_0. In the following, we make further observations of the effect of the dispersion parameter μ on the amplitude of the resulting leading wave. For this reason, we performed a simulation with a

Gaussian landslide moving at constant speed $V = 0.5$ m/sec using several values $\mu = \{0.2, 0.25, 0.3, 0.35\}$. Wave elevation snapshots for several consecutive times are presented in Figure 6. As shown in the figure, a larger μ produces a wave with a lower amplitude. In other words, the amplitude of the waves generated by the landslide is more affected by the movement of the landslide when μ is small or when the depth of the water h_0 is relatively shallow.

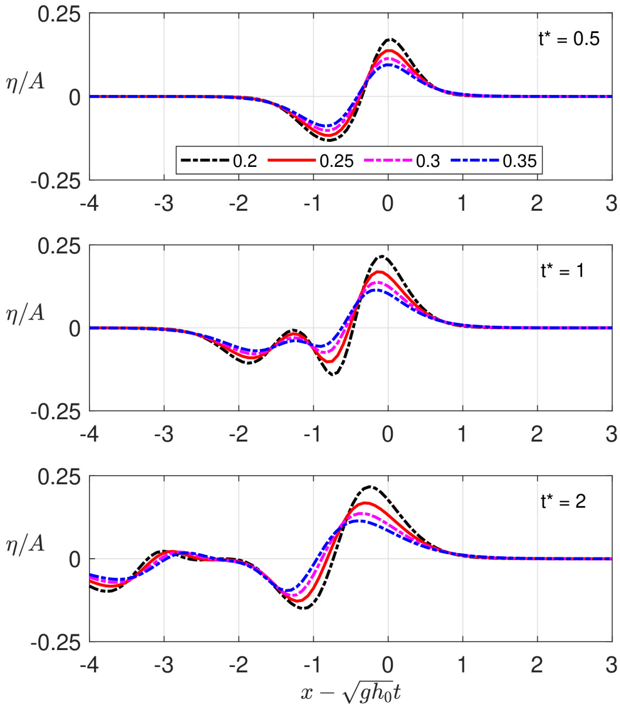

FIGURE 6. Snapshots of wave elevation $\eta(x,t)/A$ at subsequent times, generated by a Gaussian landslide moving at a constant speed $V = 0.5$ m/sec, calculated using four different depths of water $\mu = h_0/L = \{0.2, 0.25, 0.3, 0.35\}$.

5. CONCLUSIONS

In this research, waves generated by landslides are studied. The analytical solution of the full linear dispersive model expressed in terms of the inverse Fourier and Laplace transforms is adopted. We have simulated the emergence of a free surface wave due to a landslide propagating over a constant depth; various shapes of landslides that moved with constant velocity were tested. Further, we showed that various shapes of landslides with the same enclosed area generated free surface waves with the same leading wave; and this is to confirm the predictions from the far-field theory. Moreover, landslide movement has a stronger impact on the amplitude of landslide-generated waves when the depth is relatively shallow.

Acknowledgement. The authors thank Dede Tarwidi for fruitful discussions at the initial stage of this research.

REFERENCES

[1] S. Tinti, E. Bortolucci, and C. Chiavettieri, "Tsunami excitation by submarine slides in shallow-water approximation," *Pure and Applied Geophysics*, vol. 158, pp. 759–797, 2001. https://doi.org/10.1007/PL00001203.

[2] C. Whittaker, R. Nokes, and M. Davidson, "Tsunami forcing by a low froude number landslide," *Environ Fluid Mech*, vol. 15, pp. 1215–1239, 2015. https://doi.org/10.1007/s10652-015-9411-6.

[3] S. S. Tjandra and S. R. Pudjaprasetya, "Simulation of nonlinear surface waves generated by submarine landslides," *AIP Conf. Proc.*, vol. 1716, no. 1, 2016. https://doi.org/10.1063/1.4942991.

[4] I. Magdalena, K. Firdaus, and D. Jayadi, "Analytical and numerical studies for wave generated by submarine landslide," *Alexandria Engineering Journal*, vol. 61, no. 9, pp. 7303–7313, 2022. https://doi.org/10.1016/j.aej.2021.12.069.

[5] H.-Y. Lo and P. L.-F. Liu, "On the analytical solutions for water waves generated by a prescribed landslide," *Journal of Fluid Mechanics*, vol. 821, pp. 85–116, 2017. https://doi.org/10.1017/jfm.2017.251.

[6] H. Jing, G. Chen, C. Liu, W. Wang, and J. Zuo, "Dispersive effects of water waves generated by submerged landslide," *Natural Hazardz*, vol. 103, pp. 1917–1941, 2020. https://doi.org/10.1007/s11069-020-04063-z.

[7] H. Jing, Y. Gao, C. Liu, and J. Hou, "Far-field characteristics of linear water waves generated by a submerged landslide over a flat seabed," *Journal of Marine Science and Engineering*, vol. 196, pp. 1–16, 2020. https://doi.org/10.3390/jmse8030196.

[8] P. Lynett and P. L.-F. Liu, "A numerical study of submarine-landslide-generated waves and run-up," *Proceedings of the Royal Society of London*, vol. 458, pp. 2885–2910, 2002. https://doi.org/10.1098/rspa.2002.0973.

[9] P. L.-F. Liu, P. Lynett, and C. E. Synolakis, "Analytical solutions for forced long waves on a sloping beach," *Journal of Fluid Mechanics*, vol. 478, pp. 101–109, 2003. https://doi.org/10.1017/S0022112002003385.

[10] D. Tarwidi, S. R. Pudjaprasetya, and D. Adytia, "A reduced two-layer non-hydrostatic model for submarine landslide-generated tsunamis," *Applied Ocean Research*, vol. 127, p. 103306, 2022. https://doi.org/10.1016/j.apor.2022.103306.

[11] D. Tarwidi, S. R. Pudjaprasetya, and S. S. Tjandra, "A non-hydrostatic model for simulating weakly dispersive landslide-generated waves," *Water*, vol. 15, no. 4, p. 652, 2023. https://doi.org/10.3390/w15040652.

[12] K. T. Ramadan, "Near- and far-field tsunami waves, displaced water volume, potential energy and velocity flows rates by a stochastic submarine earthquake source model," *Global Journal*

of Pure and Applied Mathematics, vol. 14, pp. 649–672, 2018. https://doi.org/10.5194/nhess-2018-107.

[13] M. D. Risio, G. Belloti, A. Panizzo, and P. D. Girolamo, "Three-dimensional experiments on landslide generated waves at a sloping coast," *Coastal Engineering*, vol. 56, pp. 695–671, 2009. https://doi.org/10.1016/j.coastaleng.2009.01.009.

[14] C. C. Mei, *The Applied Dynamics of Ocean Surface Waves*. World Scientific, 1989. https://books.google.co.id/books?id=Ks82DwAAQBAJ.